HHS Public Access

Author manuscript

Phys Med Biol. Author manuscript; available in PMC 2016 December 21.

Published in final edited form as:

Phys Med Biol. 2015 December 21; 60(24): 9203–9213. doi:10.1088/0031-9155/60/24/9203.

Kilovoltage radiosurgery with gold nanoparticles for Neovascular Age-Related Macular Degeneration (AMD): a Monte Carlo evaluation

D. Brivio[1], **P. Zygmanski**[1], **M. Arnoldussen**[2], **J. Hanlon**[2], **E. Chell**[2], **E. Sajo**[3], **G. M. Makrigiorgos**[1], and **W. Ngwa**[1,3]

[1]Brigham & Woman's Hospital, Boston, MA, Dana Farber Cancer Institute, Boston, MA, Harvard Medical School

[2]Oraya Therapeutics, Inc., Newark, California 94560

[3]University of Massachusetts at Lowell, MA

Abstract

This work uses Monte Carlo radiation transport simulation to assess the potential benefits of gold nanoparticles (AuNP) in the treatment of Neovascular Age-Related Macular Degeneration (AMD) with stereotactic radiosurgery. Clinically, a 100 kVp X-ray beam of 4 mm diameter is aimed at the macula to deliver an ablative dose in a single fraction. In the transport model, AuNP accumulated at the bottom of the macula are targeted with a source representative of the clinical beam in order to provide enhanced dose to the diseased macular endothelial cells. It is observed that, because of the AuNP, the dose to the endothelial cells can be significantly enhanced, allowing for greater sparing of optic nerve, retina and other neighboring healthy tissue. For 20 nm diameter AuNP concentration of 32 mg/g, which has been shown to be achievable *in vivo*, a dose enhancement ratio (DER) of 1.97 was found to be possible, which could potentially be increased through appropriate optimization of beam quality and/or AuNP targeting. A significant enhancement in dose is seen in the vicinity of the AuNP layer within 30 um, peaked at the AuNP-tissue interface. Different angular tilting of the 4 mm-beam results in a similar enhancement. The DER inside and in the penumbra of the 4 mm irradiation-field are almost the same while the actual delivered dose is more than one order of magnitude lower outside the field leading to normal tissue sparing. The prescribed dose to macular endothelial cells can be delivered using almost half of the radiation allowing reduction of dose to the neighboring organs such as retina/optic nerve by 49% when compared to a treatment without AuNP.

1. INTRODUCTION

Age-Related Macular Degeneration (AMD) (NEI 2015) is a common eye disease which causes vision loss in people older than 50 years, due to damage to the macula. Choroidal neovascular (wet) AMD can be treated with injections of anti-Vascular Endothelial Growth Factor (anti-VEGF) drugs into the eye, but real-world outcomes have shown that mean vision gains from such mono-therapeutic strategy may persist for only 1 to 3 years (Holz et al. 2015; Tufail 2014). Photodynamic therapy and laser photocoagulation are alternate treatments that can seal the abnormal blood vessels, but are typically considered secondary

since they are not as efficacious as anti-VEGF mono-therapy. Unfortunately, the above therapies do not result in a complete cure of the disease. The condition may progress even with treatment.

Kilovoltage radiosurgery for wet AMD has been proposed as an adjunct to anti-VEGF therapy and developed by Oraya Therapeutics, Inc. (Hanlon et al. 2009; Hanlon et al. 2011) to preserve vision while simultaneously reducing the need for injections. The Oraya radiotherapy (IRay) system holds and controls eye motion while irradiating the macula with two or three 100 kVp beams tilted at a nominal polar angle θ of 30° and with possible azimuthal angles ϕ of 150°, 180° and 210° (see experimental setup in Fig. 1). The spot size of the beams is 3.5 mm upon sclera entry and 4 mm at the retina. Each beam delivers either 5.33 Gy or 8 Gy to the macular endothelial cells for a total of 16 Gy. The system includes an eye stabilization and tracking device (the 'I-Guide'), on-board imaging, and motion management software. The I-Guide consists of a suction-enabled scleral lens that is applied to the eye, retro reflective fiducials for tracking eye position and gaze angle, and a stabilizer bar that mounts to the system table. The imaging system uses two cameras to determine range and XY orientation of the IRay to the I-Guide fiducials, and the motion management software monitors targeting accuracy. During treatment, the I-Guide fiducials are tracked and the x-ray beam's position is calculated to ensure accurate targeting and avoidance of sensitive structures. If there is excessive eye motion, the beam is gated-off, and treatment resumed after appropriate system realignment. The radiation delivery requires less than 6 min of beam time, with a typical procedure lasting about twenty minutes. Wet AMD causes vision loss due to leaky vascular endothelial cells which rapidly proliferate. This radiosurgical therapy aims to destroy these immature vessels while minimizing the delivered dose to healthy tissues of the eye.

Gold nanoparticles (AuNP) are known to enhance local radiation dose (Berbeco et al. 2011; Ngwa et al. 2012b; Ngwa et al. 2013; Ngwa et al. 2010), especially for kV-energy photons, which is also employed by the Oraya Therapy IRay System (Ngwa et al. 2014). Targeted delivery of AuNP to the diseased choroidal endothelial cells via intravenous, periocular routes or direct injection is, thus, a prospective means to increase the therapeutic efficacy. In *in-vivo* studies Gold nanoparticles can be functionalized to specifically bind the surface of disease endothelial cells using targeting moieties such as arginine-glycine-aspartic acid (RGD) peptide enabling as described in references (Ngwa et al. 2014; Berbeco et al. 2011). The simulation shown in this study with such targeted GNP at the bottom or surface of the endothelial cell represents a more conservative scenario as described in these references. Active targeting has already been used in recent mouse studies, where intravenously administered functionalized nanoparticles could specifically target the neovascular AMD endothelial cells but not to the control eye (see (Takeda et al. 2009; Salehi-Had et al. 2011; Singh et al. 2009)).

This study investigates the potential benefits gained by the application of AuNP in the treatment of wet age-related macular degeneration with stereotactic ocular radiotherapy using the Oraya Therapy system. High spatial resolution (50 nm) Monte Carlo radiation transport is performed for tilted 4 mm diameter 100 kVp beams. Absolute dose inside and out-of-field doses are computed to evaluate the benefit of AuNPs in the target for various

levels of AuNP concentrations. In addition, a heuristic formula is derived for dose enhancement as a function of AuNP concentration, which could be incorporated into treatment planning.

2. MATERIALS AND METHODS

In this study we used the Monte Carlo N-Particle transport code MCNP6, developed at Los Alamos National Laboratory (LANL 2013). This is a recently released version of MCNP, in which we took advantage of its ability to set the cutoff energy to 1 eV for photons and to 10 eV for electrons. Electrons are transported by the usual condensed history algorithms down to 1 keV and then by a newly implemented single-event method below that energy. In this work we selected a cut off energy of 1 eV for photons and 20 eV for electrons. We selected a cutoff energy above the 10 eV limit allowed for electrons in order to avoid running out of energy-loss-inducing processes which occur close to this energy. The contribution of this further transport of 20 eV electrons is far beyond the purpose of this paper. Furthermore, unlike previous MCNP versions, which considered only K-shell and average L-shell transitions, MCNP6 addresses the full detailed photon-induced relaxation cascade, sampling all allowed transitions down to the photon and electron energy cutoffs. Although relaxation from electron-induced vacancies is still not implemented, it does not have significant dosimetric consequence in this study, as the electro-ionization cross sections of secondary electrons are much lower than the photoelectric absorption cross sections.

2.1 Geometry

A preliminary study was performed with a simplified geometry where a AuNP layer (10–100 nm) was placed at 2.4 cm depth (considered as the typical eye axial length in adults) in a $3\times3\times6$ cm^3 water rectangular parallelepiped as depicted in Figure 1 (left). This layer was modeled using various concentrations of AuNP, ranging from 5.5 mg/g – 491 mg/g of endothelial cell (volume $10\times10\times2$ μm^3). The x-ray source used in this study was a 100 kVp 4mm diameter non-divergent beam tilted 0°–30° with respect to the surface normal in the Y–Z plane. In addition, we also modeled a detailed eye geometry as seen in Figure 1 (right), which is based on the eye model of Asadi (Asadi et al. 2014) with macula and optic nerve positioning as in (Hanlon et al. 2009), and several adjustments as follows (dimensions in cm unless otherwise specified):

- vitreous chamber (sphere centered in O(0,0,0) and radius r = 0.93 cm)
- Retina (spherical shell centered in O(0,0,0) and radius 0.93 cm < r < 1.03 cm)
- Choroid (spherical shell centered in O(0,0,0), radius 1.03 < r < 1.13 cm)
- Sclera (spherical shell centered in O(0,0,0), radius 1.13 < r < 1.23 cm)
- Lens (ellipsoid centered in (0,0,0.77) and diameters (1, 1.15, 0.64))
- Skull Bone (sphere shell centered in O(0,0,0) and radius 3.505 < r < 4.05 cm)
- Anterior chamber (ellipsoid centered in (0,0,0.73) and semi diameters (0.8, 0.79, 0.78))
- Cornea (Ellipsoid centered in (0,0,0.73) and semi diameters (0.88, 0.85, 0.81))

- Optic nerve shell (cylinder radius 0.16 < r < 0.48 tilted by 19.4° with axis passing by the origin). Angle chosen to match the 3.3 mm distance from the geometric axis (see Fig 4A. (Hanlon et al. 2009))
- Optic nerve (cylinder radius r = 0.16 tilted by 19.4° with axis passing by the origin)
- Macula (cylinder radius r = 0.2 cm thickness 0.5 mm). Shifted by (x = −0.5 mm, y = 1.25 mm) from the geometric axis (see fig 4A. (Hanlon et al. 2009))
- Endothelial cell layer (cylinder radius r = 0.2 cm thickness 2 um) placed at the bottom of the macula
- AuNP layer (cylinder radius r = 0.2 cm thickness 20–100 nm) placed at the bottom of endothelial cells
- Tissue below the AuNP layer (cylinder radius r = 0.2 cm thickness 0.7 mm)

2.2 AuNP layer model

A planar cluster of AuNPs was modeled as a mixture of gold and water in a layer of thickness φ= 10–100 nm placed at the bottom of a 10×10×2 μm^3 endothelial cell (see Figure 1 (left)). For the purpose of analysis and modeling of concentration dependent DER, we defined the following type of concentrations:

- Layer concentration is defined as the total mass of gold within the AuNP layer (cluster) per its total mass including surrounding water in the layer

  $c_{Layer} = \frac{m_{Au}}{m_{Au} + m^{L}_{H_2O}}$
- Cellular concentration is defined as the total mass of gold in the AuNP cluster adhering to the cell per cell mass $c_{cell} = \frac{m_{Au}}{m_{Au} + m_{cell}} = \frac{c}{1+c}$, where c is a defined as $c = \frac{m_{Au}}{m_{cell}}$, and is the clinically relevant parameter.

Where m_{Au} is the mass of Gold in the AuNP cluster adhering to macula endothelial cells, m^{L}_{H2O} is the mass of water in the AuNP layer and m_{cell} is the mass of the endothelial cell above the AuNP layer. These concentrations are dependent on the number, N, and on the diameter, φ, of the AuNPs. The layer concentration is useful to understand the maximum number of AuNP we can place in a single layer before saturation, *i.e.* $1.9 \cdot 10^6$ for 10 nm (diameter) AuNPs, $4.8 \cdot 10^5$ for 20 nm AuNPs and $1.9 \cdot 10^4$ for 100 nm AuNPs. The non-normalized cellular concentration c is clinically relevant, but it is meaningless above an upper limit since it diverges: for instance, above concentrations higher than 100 mg/g. The cellular concentration c_{cell} is used for the empirical model below (see eq. 1) because it is conveniently normalized such that it is 1 for $m_{Au} \gg m_{cell}$. It is worthwhile to note that $c_{cell} \approx c$ for small concentrations (< 50 mg/g). We will refer to clinically relevant concentration c throughout the manuscript except in the analysis of the DER as a function of the concentration (eq. 1 and Figure 3) since it involves high concentration values. For 100 nm diameter AuNP, a concentration c=32 mg/g corresponds to around 600 AuNPs/cell, while 8×10^4 AuNPs/cell are needed to get the same concentration for 20 nm diameter.

In the present simulation self-absorption of electrons within AuNP was not evaluated since we modeled a water-gold mixture. Self-absorption becomes important when the AuNP size approaches electron range in gold which is an energy dependent parameter (e.g. on the order of 400nm for electron energy of 10keV and 2.2 μm for energy of 30keV (Berger et al. 2011)). For 100nm AuNP and 100kVp photons the self-absorption is expected to reduce the number of escaping electrons by about 10–15%, while for 20nm AuNP their number would be reduced by about 5% (Lechtman et al. 2011; McMahon et al. 2011). The greatest impact of self-absorption will be seen for low energy electrons in large AuNPs, which cannot escape from the AuNP.

3. RESULTS

3.1 Water parallelepiped results

In order to evaluate the main dosimetric features we first studied the behavior of a simple rectangular parallelepiped of water under irradiation of a 4 mm, 100 kVp non-divergent x-ray beam. We placed the AuNP layer at 2.4 cm depth (typical adult eye anterior to posterior diameter) and scored the energy deposited in voxels with cylindrical symmetry. In the radial direction the voxels are annuli with a central disk of 0.1 cm radius and several rings with external radii of 0.15, 0.2, 0.25, 0.3, 0.35, 1.35 cm, while along the z direction the thickness of the cylinder/rings goes from 0.1 cm down to 50 nm close to the AuNP layer. AuNP diameters of 10, 20 nm and 100 nm were considered. For 100 nm AuNPs with c=491 mg/g, dose as a function of depth is shown in figure 2 (Left) for different radial annuli and a zoom of the same dose close to the AuNP layer as a function of distance from gold is depicted with solid lines in Figure 2 (Right) and compared to the case without AuNP (dashed lines). This concentration and size of AuNPs was chosen to highlight the enhancement and decay behavior close to the AuNP interface. The 100 kVp photon source was a disk of 0.2 cm radius. The dose within this size is exactly the same (0.1 cm disk or 0.15 cm and 0.2 cm annuli). Notice that the dose in the external annuli ($r > 0.2$ cm in Figure 2 (Left)) increases in the first cm and then gradually decreases. This behavior is due to the scattering of radiation from the central beam by water molecules. This scattered radiation gives rise to dose enhancement close to the AuNP layer also in the external annuli (Figure 2 (right)).

Dose Enhancement Ratio (DER) is defined as the ratio of doses with and without AuNP. The DER is computed in small regions of the eye. For 100 nm AuNPs, the DER as a function of distance from the AuNP layer for different concentrations is shown in Figure 3 (left). On the right in Figure 3 we show the DER as function of AuNP concentration within a disk of 4 mm diameter and 2 um thickness (Macular endothelial cells volume) up and downstream respect to the x-ray beam direction. The upstream value is the most important for treatment, since the AuNP layer is placed below the macula. In the case the AuNP are delivered via active targeting they will be below the targeted endothelial cells. This is the reason for considering the upstream value the most relevant. The downstream DER will affect mainly the 20um region inside the blood vessels and it is considered less relevant because of blood flow.

Solid lines represent the following empirical model of the DER dependence on the concentration

$$DER(c_{cell}) = (1 - (c_{cell}/c_{cell,\max}))^{p} + (c_{cell}/c_{cell,\max})^{q} \cdot D_{Au}/D_{H_2O}, \quad (1)$$

This model allows the prediction of the DER for various concentrations of AuNP ($c_{cell,max}$ is the value of cellular concentration when a slab made of pure gold is placed instead of the AuNP cluster). D_{Au} and D_{H2O} are respectively the dose in the above-mentioned volume when AuNP layer is substituted by a gold slab and a water layer; p and q are unit-less parameters found by fitting the DER (c_{cell}) formula to the simulation data (upstream p=5.77452, q=0.976113; downstream p=6.43615, q=0.988021). Formula (1) may be useful in treatment planning process which uses sub-mm dose calculation grid rather than nm-grid, for example in estimating the effective dose received by the macular endothelial cells of a specific patient given the AuNP concentration delivered.

Since the delivery of AuNP is critical in these simulations we evaluated the worst case placing AuNP not only in the targeted area but also in the surroundings with the same concentration. The irradiation field and the irradiation focal point is much more under control with the IRay system developed by Oraya Therapeutics. While DER is almost constant inside and outside the irradiation field (see Figure 4 left), the absolute dose decreases more than one order of magnitude outside the beam (Figure 4 right), which is reassuring in cases AuNP are also outside the target area. The vertical line at 0.2 cm in Figure 4 represents the border of the irradiation field. The slight increase and decrease of the DER in the region outside of the field visible in Figure 4 (left) may be explained by (off-axis distant dependent) spectral changes of the incoming 100 kVp beam due to scattering (Tsiamas et al. 2014). Electron emission by gold is higher for a beam with larger spectral components around 20–40 keV with consequent larger dose enhancement. The out of field behavior is remarked also in Figure 5 with the Off Axis Ratio as function of radial distance from the center of the field. The case of 100 nm AuNPs with concentration of 32 mg/g, which has been shown to be achievable *in vivo* (Kang et al. 2009), is shown in Figure 5, together with the case of just water (*i.e.* no AuNP). The profile is shown for few distances from the AuNP layer (placed at 2.4 cm depth) along the beam propagation axis: the value at −2.4 cm corresponds to water surface, while the one at −2 μm corresponds to the macular endothelial cell thickness. Off Axis Ratio (OAR) is defined as

$$OAR(z, r) = \frac{Dose(z, r)}{Dose(z, r=0)}; \quad (2)$$

As shown in Figure 5 the OAR outside of the field increase as the depth in water increase because of x-ray scattering from the surrounding water. The OAR with and without AuNP are almost the same, this shows that the presence of AuNP increase the dose outside the field of about the same factor (DER) of the dose inside the field. As evident in Fig. 4 (right) and Fig. 5 the radial dose distribution drops from 100% to about 5% in 0.5 mm. The penumbra region, defined as the 80%-to−20% dose falloff, is therefore less than 0.5 mm.

DER has been found independent of the irradiation angle. Figure 6 depicts the DER within a disk of 4 mm diameter (macular dimension) for 32 mg/g and 0°, 10°, 30° tilt angles as function of the distance Δz from the AuNPs layer (vertical orange lines). In the tilted cases

we divided the radial disks and annuli in half (left/right half in Figure 6) perpendicularly to the plane defined by the beam and the z-axis in order to evaluate the effect of the tilting of the beam on two portion of the macula.

The asymmetry in the profile shown in Figure 6 is consistent with the asymmetric emission of photo-electrons by gold atoms (larger in the direction of the x-ray beam).

3.2 Eye geometry result

Considering the eye geometry depicted in Figure 1 (Right), we evaluated the potential benefit of wet AMD treatment with 20 nm diameter AuNPs in terms of reduced dose on surrounding healthy tissues such as the retina, optic nerve, lens, etc. The effect of a AuNP layer spread in the radial direction few cm larger than the x-ray field has been studied in the parallelepiped geometry. Here we considered an AuNP 4 mm-disk layer, 20 nm thick with concentration of 32 mg/g, which has been shown to be achievable *in vivo*, placed at the bottom of macula. We simulated irradiation using a 4 mm 100 kVp non divergent beam positioned following these steps:

- Beam alignment along the eye's axis of symmetry
- Beam transposing to target the macula (shifted of x=−0.5 mm and y=1.25 mm as described in Figure 4A of (Hanlon et al. 2009))
- Beam tilting by nominal angle 30° (real angle: θ=31.17°, ϕ=−1.28°)

We found a DER of 1.97+/−0.03 in macular endothelial cells (error after 5E8 histories simulated, standard deviation is only for statistical accuracy). The AuNP allows treating the macular endothelial cells with almost half of the ionizing radiation to the surrounding healthy tissues, while providing the same prescribed dose thanks to the energy deposited by photo- and Auger electrons. Consequently, the endothelial cells receive the prescribed dose while the organs at risks will receive the following dose reduction rate defined as

$$DRR=1-\frac{D_{AuNP}^{organ\ at\ risk}}{D_{H_2O}^{organ\ at\ risk}}\cdot\frac{D_{H_2O}^{Endothelial\ cells}}{D_{AuNP}^{Endothelial\ cells}},$$ where D_{AuNP} and D_{H2O} are respectively the doses with and without AuNP in the organ/tissue mentioned in the superscript:

- Lens: DRR = 0.492
- Optic nerve: DRR = 0.492
- Non-targeted Macula above the AuNP layer: DRR = 0.490
- Non-targeted tissue below the AuNP layer: DRR = 0.488

The slight difference in DRR in the different tissues is due to the more or less vicinity to the AuNP layer and to the slight difference in material densities.

4. DISCUSSION AND CONCLUSIONS

We evaluated the potential benefit of AuNPs in the treatment of neovascular Age-related Macular Degeneration with 100 kVp radiosurgery. We found that a dose enhancement of 1.97 can be obtained with an in-vivo feasible 20 nm AuNP concentration of 32 mg per gram

of endothelial cells. In this paper we also studied the behavior of the DER in the macular endothelial cells as a function of AuNP concentration and we developed an intuitive empirical model for DER prediction based on the fit of Monte Carlo simulation outcomes. A small concentration as low as 5 mg/g contribute to a dose enhancement of about 15%. We focused on a nanoparticle concentration of 32 mg/g which has been safely employed in mice *via* subconjunctival injection in the eye (Kang et al. 2009). In this paper we also showed that higher DER and sparing of healthy tissue will be obtained employing higher AuNP concentrations (Fig. 3).

The results of this MC simulation provide further confirmation of the potential to increase DER with AuNP from previous analytical calculations (Ngwa et al. 2012a). The clinical feasibility of AuNP targeting of macular endothelial cells via direct injection or via periocular routes must be addressed in experimental studies since the AuNP location is critical to obtain the desired dose enhancement. Preliminary *in-vivo* studies in mice already show feasibility (see (Takeda et al. 2009; Salehi-Had et al. 2011; Singh et al. 2009)). This is promising but this still have to be shown in humans. The results of this simulation can be easily extended to the radiotherapy treatment of other ocular diseases like retinoblastoma and choroidal melanoma whose endothelial cells can also be precisely targeted with AuNP.

AuNP are particularly attractive as they have also been shown (Kim et al. 2011) to inhibit retinal neovascularization in mice *via* suppression of VEGFR-2 signaling pathway and can be safely applied to the retina. Hence the benefit of their use could go beyond providing dose enhancement. Kim et al. found that the number of vascular lumens using 1μM of 20nm AuNP was reduced by a factor of 3. Experimental studies are needed to optimize such potential benefits.

Preliminary results for mono-energetic x-ray beams suggest a path for DER and percent depth dose improvement, by modifying the radiation spectrum. Compared to 100 kVp, usage of filtered spectra with enhanced flux in the region 20 keV–40 keV shows further increase of DER. This could pave the way for further improvement of radiotherapy treatment effectiveness for wet AMD, but requires further studies. In particular, optimization of x-ray source/spectra, in addition to dose enhancement ratio (DER), and skin-to-tumor dose ratio has to be considered (Tsiamas et al. 2014). While in general softening of spectrum increases DER, at the same time it decreases the penetration of the beam. For ocular geometry (depths of less than 3 cm) low x-rays energies can be utilized, but even in this case, due to attenuation, the useful energy limit is about 20 keV (lower bound).

In conclusion, this study provides impetus to improve treatment effectiveness of radiotherapy of wet AMD by targeting macular endothelial cells with gold nanoparticles. By using Monte Carlo simulations we showed that a significant dose enhancement to the endothelial cells can be obtained and consequently the dose to the organs at risks can be reduced. This type of treatment may help patients with AMD to preserve vision reducing at the same time the need of anti-VEGF injections every few years.

Acknowledgments

This work was supported by NIH R41EY024197.

References

Asadi S, et al. Gold nanoparticles-based brachytherapy enhancement in choroidal melanoma using a full Monte Carlo modelling of human eye. 2014 ArXiv ID: 1406.4334v2.

Berbeco RI, Ngwa W, Makrigiorgos GM. Localized dose enhancement to tumor blood vessel endothelial cells via megavoltage X-rays and targeted gold nanoparticles: new potential for external beam radiotherapy. Int J Radiat Oncol Biol Phys. 2011; 81(1):270–276. [PubMed: 21163591]

Berger, MJ., et al. ESTAR : Stopping-Power and Range Tables for Electrons, Protons, and Helium Ions. NIST. 2011. http://www.nist.gov/pml/data/star/index.cfm

Hanlon J, et al. Kilovoltage stereotactic radiosurgery for age-related macular degeneration: Assessment of optic nerve dose and patient effective dose. Medical Physics. 2009; 36(8):3671. [PubMed: 19746800]

Hanlon J, et al. Stereotactic radiosurgery for AMD: A monte carlo-based assessment of patient-specific tissue doses. Investigative Ophthalmology and Visual Science. 2011; 52(5):2334–2342. [PubMed: 21087954]

Holz FG, et al. Multi-country real-life experience of anti-vascular endothelial growth factor therapy for wet age-related macular degeneration. Br J Ophthalmol. 2015; 99:220–226. [PubMed: 25193672]

Kang SJ, et al. Subconjunctival nanoparticle carboplatin in the treatment of murine retinoblastoma. Archives of ophthalmology. 2009; 127(8):1043–1047. [PubMed: 19667343]

Kim JH, et al. The inhibition of retinal neovascularization by gold nanoparticles via suppression of VEGFR-2 activation. Biomaterials. 2011; 32(7):1865–1871. [PubMed: 21145587]

LANL. MCNP6 version 1.0, released in 2013. Los Alamos National Laboratories; 2013. Available at: https://rsicc.ornl.gov/

Lechtman E, et al. Implications on clinical scenario of gold nanoparticle radiosensitization in regards to photon energy, nanoparticle size, concentration and location. Physics in medicine and biology. 2011; 56(15):4631–4647. [PubMed: 21734337]

McMahon SJ, et al. Biological consequences of nanoscale energy deposition near irradiated heavy atom nanoparticles. Scientific Reports. 2011:1. [PubMed: 22355520]

NEI. National Eye Institute, Age-Related Macular Degeneration. 2015. Available at: http://www.nei.nih.gov/health/maculardegen/armd_facts.asp

Ngwa W, et al. In vitro radiosensitization by gold nanoparticles during continuous low-dose-rate gamma irradiation with I-125 brachytherapy seeds. Nanomedicine. 2013; 9(1):25–27. [PubMed: 23041410]

Ngwa W, et al. Targeted radiotherapy with gold nanoparticles: current status and future perspectives. Nanomedicine (London, England). 2014; 9(7):1063–82.

Ngwa W, Makrigiorgos GM, Berbeco RI. Applying gold nanoparticles as tumor-vascular disrupting agents during brachytherapy: estimation of endothelial dose enhancement. Phys Med Biol. 2010; 55(21):6533–6548. [PubMed: 20959684]

Ngwa W, Makrigiorgos GM, Berbeco RI. Gold nanoparticle enhancement of stereotactic radiosurgery for neovascular age-related macular degeneration. Phys Med Biol. 2012a; 57(20):6371–6380. [PubMed: 22995994]

Ngwa W, Makrigiorgos GM, Berbeco RI. Gold nanoparticle-aided brachytherapy with vascular dose painting: estimation of dose enhancement to the tumor endothelial cell nucleus. Med Phys. 2012b; 39(1):392–398. [PubMed: 22225308]

Salehi-Had H, et al. Utilizing targeted gene therapy with nanoparticles binding alpha v Beta 3 for imaging and treating choroidal Neovascularization. PLoS ONE. 2011; 6(4)

Singh SR, et al. Intravenous transferrin, RGD peptide and dual-targeted nanoparticles enhance anti-VEGF intraceptor gene delivery to laser-induced CNV. Gene therapy. 2009; 16(5):645–659. [PubMed: 19194480]

Takeda A, et al. CCR3 is a target for age-related macular degeneration diagnosis and therapy. Nature. 2009; 460(7252):225–230. [PubMed: 19525930]

Tsiamas P, et al. Low-Z linac targets for low-MV gold nanoparticle radiation therapy. Med Phys. 2014; 41(2):21701.

Tufail A. The neovascular age-related macular degeneration database: Multicenter study of 92 976 ranibizumab injections: Report 1: Visual acuity manuscript no. 2013–568. Ophthalmology. 2014; 121(5):1092–1101. [PubMed: 24461586]

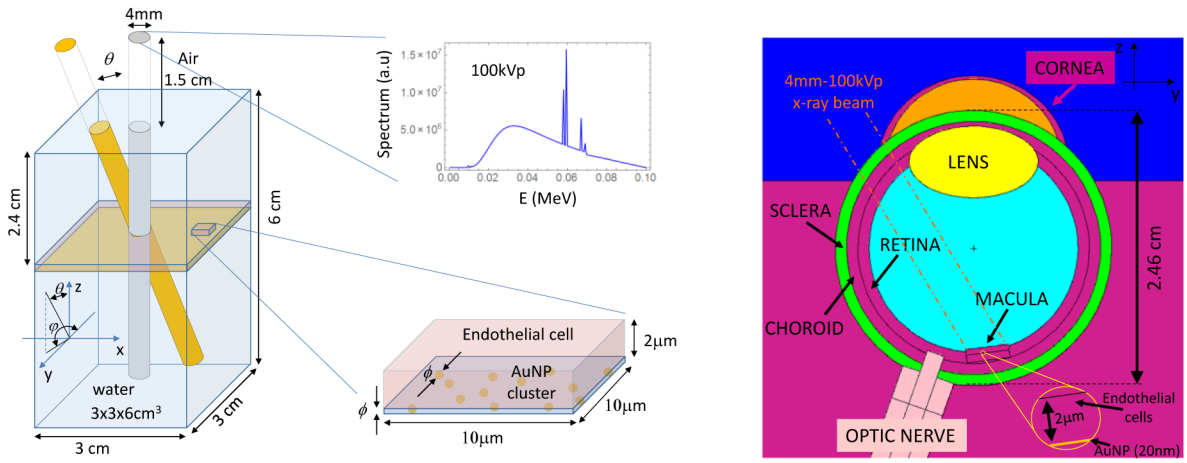

Figure 1.

(left) Simplified MC simulation geometry with the 4 mm – 100 kVp x-ray beam direction and spectrum; a zoom of the endothelial cell with at the bottom the AuNP layer is shown, (right) detailed eye geometry (YZ section), AuNP layer (20 nm) is located at the bottom of macular endothelial cells (2 μm). Neighboring organs (optic nerve, Retina, Lens, etc) and the direction of the incoming x-ray beam are depicted.

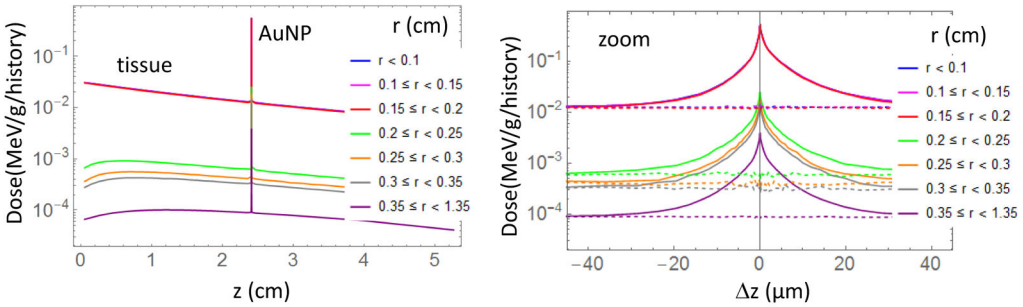

Figure 2.

(Left) Dose as function of depth for different radial annulus. 100 nm diameter AuNP layer with c=491 mg/g is placed at 2.4 cm depth (typical adult eye anterior to posterior diameter). (Right) Detail of the dose enhancement close to the AuNP layer (solid line), dashed lines represent the case without AuNP. MC uncertainties are below 1.2% for 0.1 cm disk and for 0.15 cm and 0.2 cm annuli (inside the radiation field) and below 4 % for the other annuli (outside the radiation field).

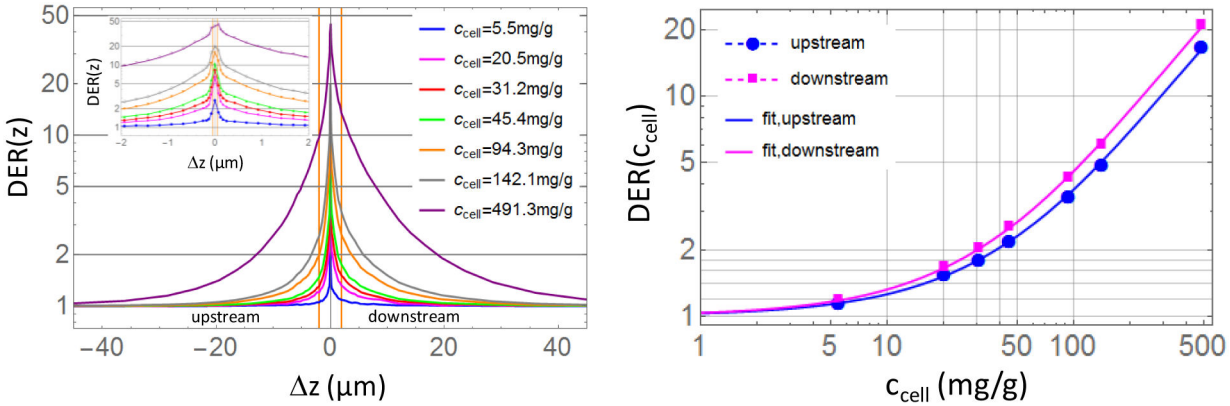

Figure 3.

(left) DER(z) for 100 nm AuNPs with different concentrations c_{cell}, orange vertical lines represents 2 um-endothelial cells size. (right) DER (c_{cell}) in 2 um layer inside a disk of 4 mm diameter (macular endothelial cells).

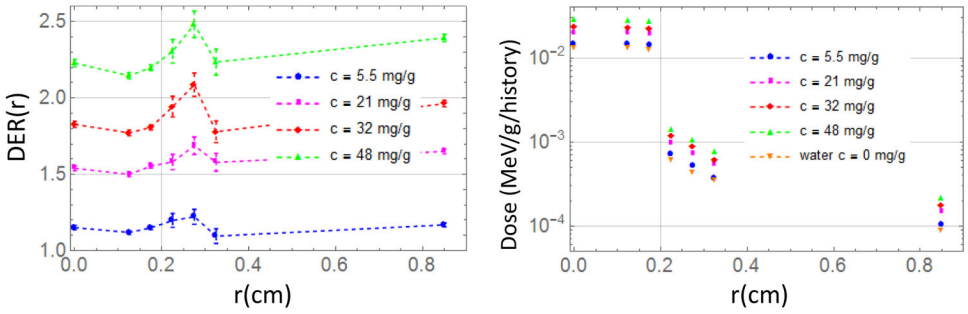

Figure 4.

DER (left) and Dose (right) as a function of the radial distance from the center of the macula for 100nm AuNP.

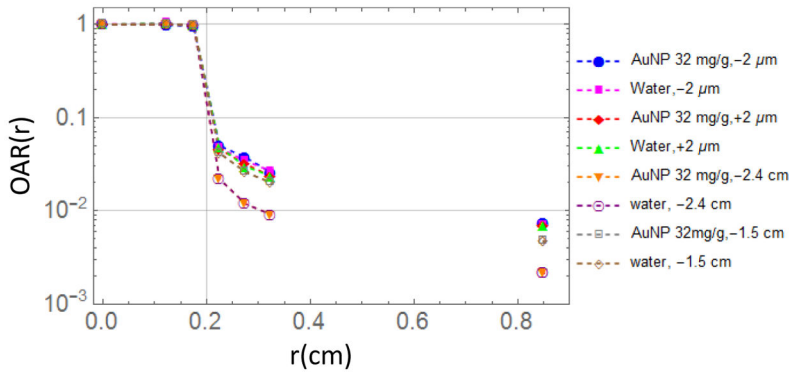

Figure 5.

Off Axis Ratio (OAR) as a function of the radial distance from the center of the macula for c=32 mg/g and for water. The profile is shown for few distances from the AuNP layer (placed at 2.4 cm depth) along the beam propagation axis: the value at −2.4 cm corresponds to water surface, while the one at −2 μm corresponds to the macular endothelial cell thickness.

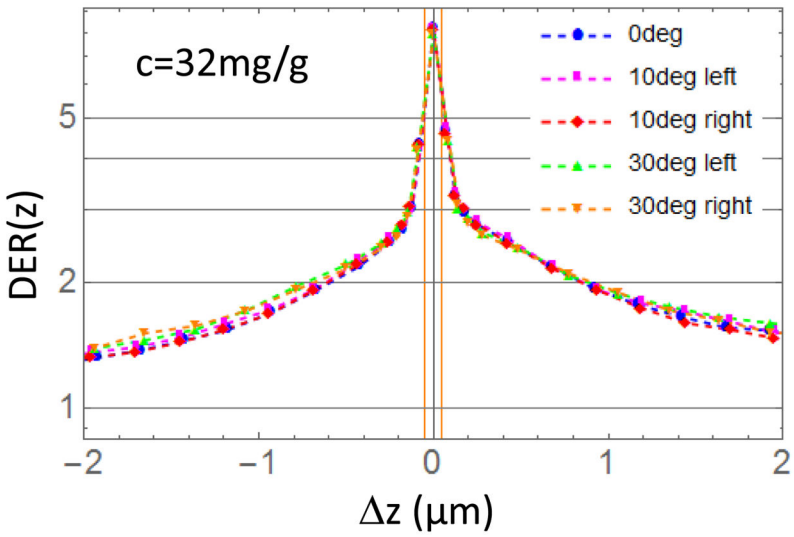

Figure 6.
DER (z) for tilted irradiation beams as a function of the distance Δz from the AuNPs layer (vertical orange lines are the surface of the AuNP layer). Left/right half correspond to cuts of the radial disk and annuli perpendicularly to the plane defined by the beam and the z-axis.